A Unified Approach to Multiuser Detection and Space-Time Coding with Low Complexity and Nearly Optimal Performance[1]

Li Ping, Lihai Liu, K. Y. Wu, and W. K. Leung
Department of Electronic Engineering, City University of Hong Kong, Hong Kong
Email: eeliping@cityu.edu.hk

Abstract

Techniques using interleaving as the basic means for signal separation are introduced for both multiple access systems and multiple transmit antenna systems. For multiple access channels, the proposed interleave-division multiple-access (IDMA) scheme can achieve near capacity performance. For multiple antenna systems, the performance of the proposed interleave-division-multiplexing space-time (IDM-ST) codes is close to the so-called canonical performance, which is a theoretical measurement of full transmit diversity. Both IDMA and IDM-ST schemes are characterized by very low receiver complexity and are inherently asynchronous.

I. Introduction

The performance of conventional CDMA systems [1]-[3] and multiple transmit antenna systems [4][5] is limited by interference, i.e., multiple access interference (MAI) for the former and cross antenna interference (CAI) for the latter, as well as intersymbol interference (ISI) for both.

The use of signature sequences for user separation is a characteristic feature for a conventional CDMA system. Interleaving, which is usually placed between forward error correction (FEC) coding and spreading, is traditionally employed to combat the fading effect. The possibility of employing interleaving for user separation in CDMA systems is briefly mentioned in [1] but the receiver complexity is considered as a main obstacle. In [6][7], a performance improvement achieved by assigning different interleavers to different users in a CDMA system is demonstrated. In [8], multiuser detection in narrowband applications with a small number of users is investigated. A bandwidth-efficient trellis coded-modulation (TCM) system is made user-specific by selecting a unique combination of trellis code structure, interleaver and modulation constellation.

This paper presents an asynchronous interleave-division multiple-access (IDMA) scheme for spread spectrum mobile communication systems, in which users are distinguished by different chip-level interleaving methods instead of by different signatures as in a conventional CDMA system. Being a wideband scheme, the proposed scheme inherits many advantages from CDMA, in particular, diversity against fading and mitigation of other-cell user interference. A very low-cost chip-by-chip iterative detection algorithm is devised. We will show that the proposed IDMA scheme can achieve performance close to the capacity of a multiple access channel.

Based on a similar principle, we present an interleave-division-multiplexing space-time (IDM-ST) coding scheme. Transmit diversity techniques based on space-time (ST) coding, such as trellis ST codes [4] and block ST codes [5], have been studied for combating fading channel impairments. Although significant progress has been made, many challenging issues related to performance and complexity remain open. In this paper, we will show that the IDM-ST scheme can achieve nearly optimal performance at very low cost in systems with an arbitrary number of transmit antennas.

For simplicity, our derivation will be based on a single-path synchronous channel model with BPSK signaling. However, both IDMA and IDM-ST schemes are inherently asynchronous (i.e., frame alignment is not a necessary condition) and can be applied to multipath channels with complex signaling constellations. We will present simulation results for these general cases.

---

[1] This work was fully supported by a grant from the Research Grant Council of the Hong Kong SAR, China [Project No. CityU 1010/01E].

II. IDMA and Multiuser Detection

A. Transmitter Structure

The upper part of Fig. 1 shows the transmitter structure of an IDMA system for the *m*th user. The encoder ENC of a low-rate code *C* is employed to produce a coded sequence $\boldsymbol{c}^{(m)}=\{c_j^{(m)}, j=1,\cdots,J\}$, where *J* is the frame length, followed by a chip level interleaver $\pi^{(m)}$ that maps $\boldsymbol{c}^{(m)}$ to $\boldsymbol{x}^{(m)}=\{x_j^{(m)}, j=1,\cdots,J\}$. We follow the convention of CDMA and call the basic elements in $\boldsymbol{c}^{(m)}$ and $\boldsymbol{x}^{(m)}$ "chips". *C* can be either the same or different for different users. It can be an FEC code, or a spreading sequence (spreading is in fact a special form of coding), or a combination of the two. From a performance point of view, it is advantageous to use a low-rate FEC code [9][10] that can provide an extra coding gain.

The key principle of IDMA is that the interleavers $\{\pi^{(m)}\}$ should be different for different users. We assume that the interleavers are generated independently and randomly.

For simplicity, we first consider time-invariant single-path channels with real channel coefficients and BPSK signaling. We will briefly outline the treatments of more general situations in II.E.

After sampling at chip rate, the received signal from *M* users can be written as

$$r_j = \sum_{m=1}^{M} h^{(m)} x_j^{(m)} + n_j, \qquad j = 1, 2, \ldots, J, \qquad (1)$$

where $x_j^{(m)}$ is the *j*th chip transmitted by the *m*th user, $h^{(m)}$ the channel coefficient for the *m*th user and $\{n_j\}$ samples of a zero-mean additive white Gaussian noise (AWGN) with variance $\sigma^2=N_0/2$.

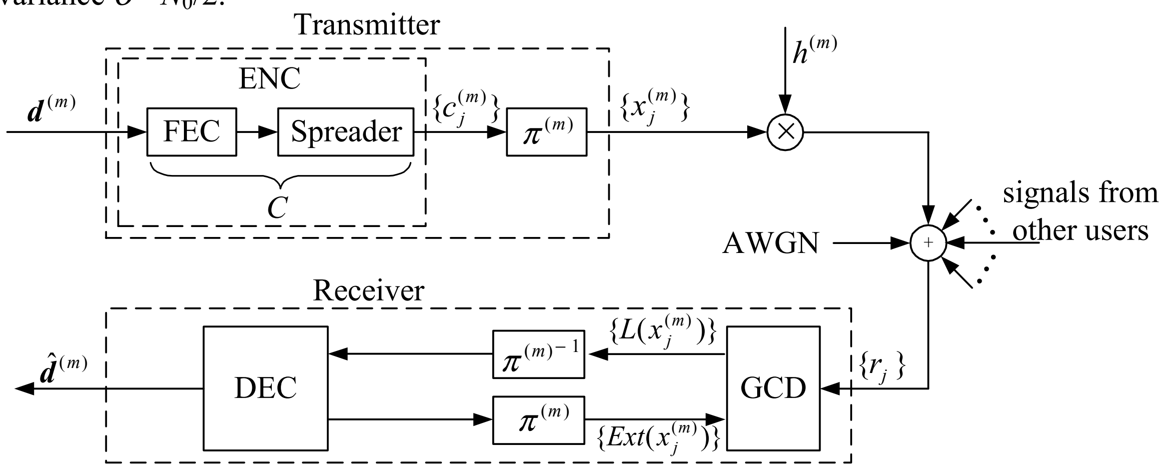

Fig. 1. Transmitter and receiver structures of the IDMA system, where $\pi^{(m)}$ is the interleaver of the *m*th user.

B. Receiver Structure

The lower part of Fig. 1 illustrates an iterative IDMA multiuser detector. It employs a low-cost chip-by-chip detection strategy and avoids conventional MAP [1][2] or matrix operations [3]. The receiver consists of a Gaussian chip detector (GCD) and an *a posteriori* probability (APP) decoder (DEC). The GCD exchanges information with the DEC in a turbo-type manner [11]. The DEC also produces hard decisions $\{\hat{\boldsymbol{d}}^{(m)}\}$ on information bits $\{\boldsymbol{d}^{(m)}\}$ in the final iteration. In the Appendix, the principle of the iterative process is further explained using Tanner graphs.

The receiver operation is based on the received signal $\boldsymbol{r} \equiv \{r_j, j = 1, \ldots, J\}$, the channel coefficients $\boldsymbol{h} \equiv [h^{(1)}, \ldots, h^{(m)}, \ldots, h^{(M)}]$ and the code constraint *C*. Finding an optimal solution is usually prohibitively complicated. We now consider a sub-optimal approach by first separating the conditions, i.e., $\boldsymbol{r}$, $\boldsymbol{h}$ and C, and then combining the results using an iterative process. This greatly reduces the complexity involved.

Specifically, the constraint of C is ignored in the GCD. The output of the GCD $\{L(x_j^{(m)}), j=1,\cdots,J, m=1,\cdots,M\}$ is defined by the logarithm likelihood ratio (LLR)

$$L(x_j^{(m)}) = \log\left(\frac{p(r_j \mid x_j^{(m)}=+1,\boldsymbol{h})}{p(r_j \mid x_j^{(m)}=-1,\boldsymbol{h})}\right), \qquad \forall\, m, j. \tag{2}$$

The DEC consists of M local APP decoders. The mth local APP decoder performs an APP decoding of C for the mth user using $\boldsymbol{L}^{(m)} = \{L(x_j^{(m)}), j=1,\cdots,J\}$ (after appropriate deinterleaving) as its input. Its output is the so-called extrinsic LLR [11]

$$Ext(x_j^{(m)}) = \log\left(\frac{Pr(x_j^{(m)}=+1 \mid \boldsymbol{L}^{(m)}, C)}{Pr(x_j^{(m)}=-1 \mid \boldsymbol{L}^{(m)}, C)}\right) - L(x_j^{(m)}), \qquad \forall\, m, j. \tag{3}$$

The APP decoding in the DEC is a standard function [11] so we will not discuss it in detail. In the following, we will focus on the GCD.

C. Detailed Descriptions of the GCD

The GCD generates coarse estimates of $\{x_j^{(m)}, j = 1, \ldots, J, m = 1, \ldots, M\}$. We ignore the constraint of C to maintain low complexity. Consider the jth chip of the mth user with $x_j^{(m)} \in \{+1, -1\}$ under BPSK modulation. We treat $x_j^{(m)}$ as a random variable and use $Ext(x_j^{(m)})$ (initialized to zero) to approximate the *a priori* LLR of $x_j^{(m)}$,

$$\log\left(\frac{Pr(x_j^{(m)}=+1)}{Pr(x_j^{(m)}=-1)}\right) \approx Ext(x_j^{(m)}). \tag{4}$$

Based on (4), we have

$$\mathrm{E}(x_j^{(m)}) \approx \frac{\exp(Ext(x_j^{(m)}))-1}{\exp(Ext(x_j^{(m)}))+1} = \tanh(Ext(x_j^{(m)})/2), \tag{5}$$

and $\mathrm{Var}(x_j^{(m)}) = 1-(\mathrm{E}(x_j^{(m)}))^2$. (6)

According to (1) and denoting $\zeta_j^{(m)} = r_j - h^{(m)}x_j^{(m)}$, the jth chip in the received signal can be expressed as

$$r_j = h^{(m)}x_j^{(m)} + \zeta_j^{(m)}. \tag{7}$$

<u>The Gaussian Approximation:</u> Applying the central limit theorem, $\zeta_j^{(m)}$ in (7) can be approximated by a Gaussian random variable with mean and variance

$$\mathrm{E}(\zeta_j^{(m)}) = \mathrm{E}(r_j) - h^{(m)}\mathrm{E}(x_j^{(m)}) \quad \text{and} \quad \mathrm{Var}(\zeta_j^{(m)}) = \mathrm{Var}(r_j) - \left|h^{(m)}\right|^2 \mathrm{Var}(x_j^{(m)}), \tag{8}$$

where (based on (1))

$$\mathrm{E}(r_j) = \sum_{m'=1}^{M} h^{(m')}\mathrm{E}(x_j^{(m')}) \quad \text{and} \quad \mathrm{Var}(r_j) = \sigma^2 + \sum_{m'=1}^{M} \left|h^{(m')}\right|^2 \mathrm{Var}(x_j^{(m')}). \tag{9}$$

Applying the Gaussian Approximation to (7) [3][12], (2) can be calculated as,

$$\begin{aligned} L(x_j^{(m)}) &= \log\frac{\exp\left(-\dfrac{(r_j-\mathrm{E}(\zeta_j^{(m)})-h^{(m)})^2}{2\mathrm{Var}(\zeta_j^{(m)})}\right)}{\sqrt{2\pi\mathrm{Var}(\zeta_j^{(m)})}} - \log\frac{\exp\left(-\dfrac{(r_j-\mathrm{E}(\zeta_j^{(m)})+h^{(m)})^2}{2\mathrm{Var}(\zeta_j^{(m)})}\right)}{\sqrt{2\pi\mathrm{Var}(\zeta_j^{(m)})}} \\ &= 2h^{(m)} \cdot \frac{r_j - \mathrm{E}(\zeta_j^{(m)})}{\mathrm{Var}(\zeta_j^{(m)})}. \end{aligned} \tag{10}$$

Then using (8), we have

$$L(x_j^{(m)}) = 2h^{(m)} \cdot \frac{r_j - \mathrm{E}(r_j) + h^{(m)}\mathrm{E}(x_j^{(m)})}{\mathrm{Var}(r_j) - \left|h^{(m)}\right|^2 \mathrm{Var}(x_j^{(m)})}. \quad (11)$$

D. A Summary of the Chip-by-Chip Detection Algorithm

For clarity, we summarize the chip-by-chip detection algorithm as follows.

Initialization: Set $Ext(x_j^{(m)})=0, \quad \forall m, j.$

Main iteration:

$$\mathrm{E}(x_j^{(m)}) \Leftarrow \tanh(Ext(x_j^{(m)})/2) \qquad \mathrm{Var}(x_j^{(m)}) \Leftarrow 1-(\mathrm{E}(x_j^{(m)}))^2, \qquad \forall m, j. \quad (12)$$

$$\mathrm{E}(r_j) \Leftarrow \sum_{m=1}^{M} h^{(m)}\mathrm{E}(x_j^{(m)}) \qquad \mathrm{Var}(r_j) \Leftarrow \sigma^2 + \sum_{m=1}^{M}\left|h^{(m)}\right|^2 \mathrm{Var}(x_j^{(m)}), \quad \forall j. \quad (13)$$

$$L(x_j^{(m)}) \Leftarrow 2h^{(m)} \cdot \frac{r_j - \mathrm{E}(r_j) + h^{(m)}\mathrm{E}(x_j^{(m)})}{\mathrm{Var}(r_j) - \left|h^{(m)}\right|^2 \mathrm{Var}(x_j^{(m)})}, \qquad \forall m, j. \quad (14)$$

The APP decoding in the DEC is performed at this point to update $\{Ext(x_j^{(m)})\}$. Then go back to (12) for the next iteration.

The normalized computational cost in (12)-(14) (excluding the APP decoding of *C*) is only 6 additions, 7 multiplications and a tanh function per chip per user per iteration. This complexity is very low and is independent of user number *M*. If *C* is a turbo-type code [10][11], the DEC may contain internal iterations. These internal iterations can be incorporated into the global iterations described above (e.g. one internal iteration per DEC per global iteration). Since other cost is so low, the overall receiver complexity is dominated by the APP decoding of *C*. The normalized cost per user is roughly the same as that of a single-user turbo decoder. For example, the complexity related to the results in Fig. 3 below is comparable to that for a standard 16-state single-user turbo decoder.

E. Generalization

The principle described above can be generalized. Some examples are listed below.

- In an asynchronous multipath channel with ISI, there may be several $\{r_j\}$ related to a transmitted chip $x_j^{(m)}$ due to multiple reflections. We can carry out (12)-(14) for each of these $\{r_j\}$ with respective to $x_j^{(m)}$ and sum up the resultant extrinsic LLRs using a rake-type operation.
- When transmitted signals and channel coefficients $\{h^{(m)}\}$ are complex, the operations (12)–(14) should be modified slightly for every chip in the real or imaginary part, but the main principle remains the same.
- For a time-varying channel, we only need to add appropriate time indexes to the channel coefficients $\{h^{(m)}\}$ in (12)-(14).

F. Simulation Results

The above detection algorithm can be carried out by either a parallel schedule (in which the operations in (12)-(14) are carried out simultaneously for all users) or a serial schedule (in which the operations in (12)-(14) are carried out user by user). The results in Figs. 2 and 3 are based on the serial schedule. We will use N_{info} for the information block length of each user, *M* for user number, *S* for the length of a spreading sequence and R_C for the rate of *C*. We define the total rate $R_{\mathrm{system}}=M\times R_C$, which is the overall measurement of the system spectrum efficiency. We observe that the structure of the spreading sequence has little impact on the IDMA performance, except that the number of +1 and –

1 should be balanced, e.g., [+1, -1, +1, -1, …]. In this section, we only consider AWGN channels where all channel coefficients are set to unit.

Fig. 2 shows the bit-error-rate (BER) performance of an uncoded IDMA schemes over AWGN channels. S = 64 (so R_C=1/64), N_{info}=256 for each user and the interleaver length is J=64×256=16384 chips. Near single-user performance is achievable for very large M. The detector converges even when M is nearly double S. (For QPSK modulation, similar performance can be achieved for twice the number of users, by splitting the signals evenly in the real and imaginary parts.)

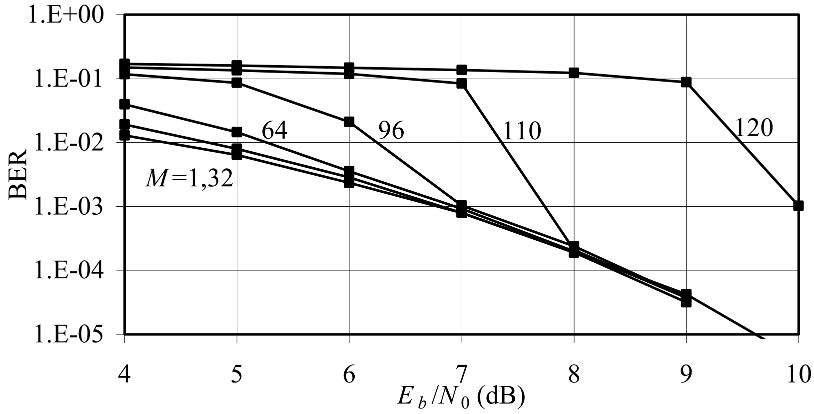

Fig. 2. Performance of uncoded IDMA schemes over AWGN channels. User number M is marked in the figure. Iteration number = 10.

Fig. 3 shows the BER performance of coded IDMA schemes over AWGN channels based on a low-rate (with rate=0.0581) turbo-Hadamard code [10] with N_{info}=4095 and S=4 (so R_C=0.014525 ≈1/69). Performance of BER=10^{-5} at $E_b/N_0 \approx$ 1.4 dB is observed with M=35 (R_{system}=0.5084). This is quite close to the capacity of a multiple access channel [13] (e.g., E_b/N_0=0 dB for R_{system}=0.5, the same as for a single-user channel).

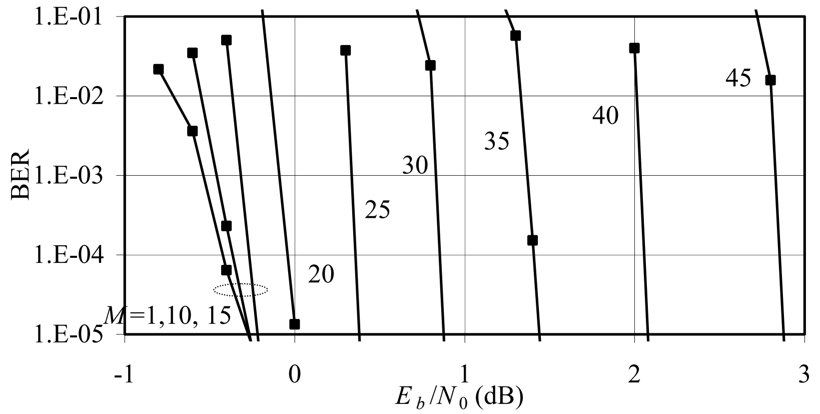

Fig. 3. Performance of an IDMA scheme based on a low-rate turbo-Hadamard code [10] over an AWGN channel. User number M is marked in the figure. Iteration number=30.

III. IDM Space-Time Codes

We now proceed to consider space-time codes. We will focus on systems with N transmit antennas and one receive antenna, referred to as N×1 systems below.

A. IDM-ST Coding Principles

Fig. 4 shows an interleave-division-multiplexing space-time (IDM-ST) coding system with N transmit antennas and one receive antenna. The information sequence $\boldsymbol{d}$ is first encoded into a stream $\boldsymbol{c}=\{c_i\}$ using a binary low-rate code C (which includes an FEC encoder and a spreader), i.e., $c_i \in \{+1, -1\}$. The encoded sequence $\boldsymbol{c}$ is then segmented into F equal-length sub-sequences $\{c^{(1)}, \ldots, c^{(f)}, \ldots, c^{(F)}\}$. To introduce randomization and increase rate, we adopt interleaving and stacking operations as follows. Each $c^{(f)}$ is independently interleaved N times, producing $\{x^{(f,n)}, n = 1, \ldots, N\}$. Altogether, we use $N\times F$ independent random interleavers. The stacking operation is defined by an ordinary linear summation,

$$X^{(n)} = \sum_{f=1}^{F} x^{(f,n)}, \qquad n=1, 2, \ldots, N. \qquad (15)$$

where $X^{(n)}$ is transmitted over the nth antenna. The stacking operation increases rate but also introduces stacking interference. However, this does not cause any additional difficulty, since stacking interference can be resolved together with CAI and ISI. F will be referred to as the stacking index. The spreader, interleavers and stackers together are referred to as an IDM-ST encoder.

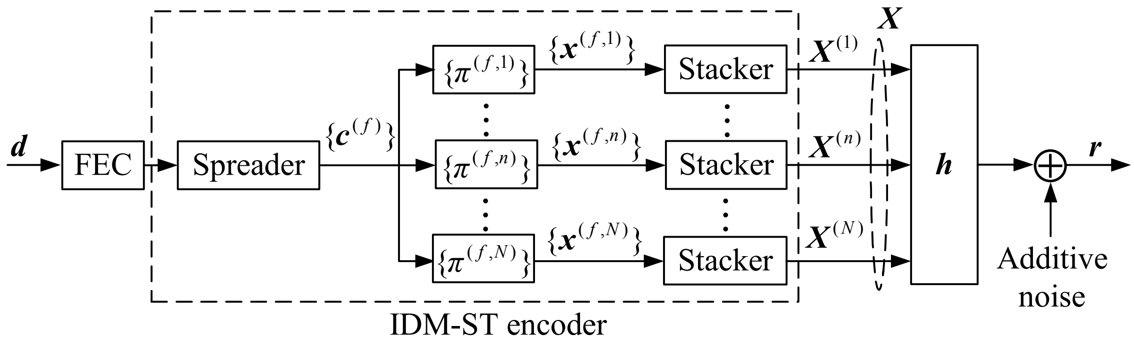

Fig. 4. An $N\times1$ IDM-ST system, where $\boldsymbol{h}\equiv[h^{(n)}]$ are the channel coefficients between the N transmit antennas and the receive antenna, and $\pi^{(f,n)}$ is the interleaver for $x^{(f,n)}$.

B. IDM-ST Receiver

The IDM-ST receiver is similar to the IDMA receiver in Fig. 1. Note that $\{x^{(f,n)}, n = 1, \ldots, N\}$ are all interleaved versions of $c^{(f)}$. (This is effectively an additional spreading operation.) The receiver still operates in a chip-by-chip manner. The basic operation is to first estimate the chips in $\{x^{(f,n)}, n = 1, \ldots, N\}$ based on (11). The LLR for a chip in $c^{(f)}$ is the sum of the LLRs of its N replicas in $\{x^{(f,n)}, n = 1, \ldots, N\}$. The computational cost of the receiver thus increases only linearly with N.

C. Canonical Performance

The capacities of an $N\times1$ channel [14][15] and a 1×1 AWGN channel [16] (with complex signaling) are respectively

$$C_{N\times1} = \log(1 + (\|\boldsymbol{h}\|^2 / N)\cdot(E_s / N_0)) \qquad \text{bits/s/Hz}, \qquad (16a)$$

$$C_{AWGN} = \log(1 + E_s / N_0) \qquad \text{bits/s/Hz}, \qquad (16b)$$

where E_s is the total average symbol energy (over all transmit antennas). According to (16), the capacities of the $N\times1$ and 1×1 systems in Fig. 5 are the same assuming equal E_s/N_0. (**Note:** E_s is based on $\boldsymbol{X}$ for the $N\times1$ system and based on $\boldsymbol{c}$ for the 1×1 system.) This motivates us to introduce the following definition.

Definition 1: The performance (e.g., BER vs. E_s/N_0) of the system in Fig. 5(a) is said to be canonical if it is the same as that of the system in Fig. 5(b) for any fixed $\boldsymbol{h}$.

Notice that in Definition 1, no assumption is made about whether the FEC code achieves capacity or not. It applies to any FEC code (including the trivial one of no coding). The system in Fig. 5(a) can achieve the capacity of $N\times1$ systems provided that

- the FEC code achieves the capacity of an AWGN channel, and
- the ST code achieves the canonical performance.

The canonical performance implies optimal diversity gain for an $N\times1$ system. It provides a convenient criterion for system performance assessment. It indicates that the FEC and ST codes can be optimized separately for coding and diversity gains respectively, which simplifies the design issue.

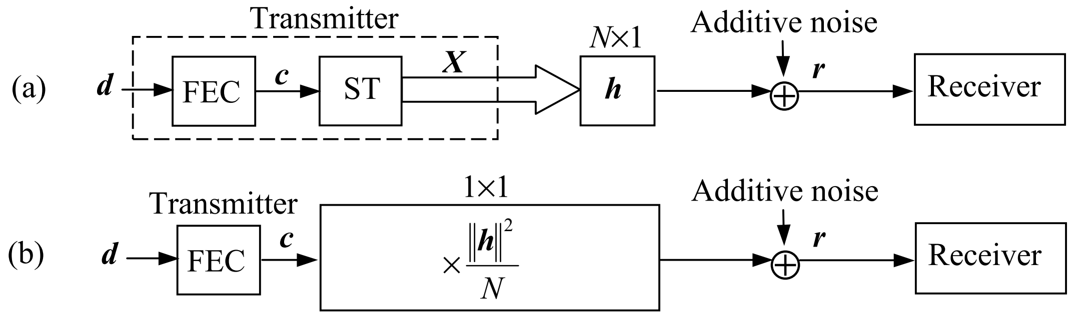

Fig. 5 (a) A generic two-stage FEC-ST system. (b) A reference 1×1 system, where a scaling factor $\|\boldsymbol{h}\|^2/N$ is applied to the transmitter output $\boldsymbol{c}$.

D. Canonical Performance in Fading Channels

The discussion above is for a fixed $\boldsymbol{h}$. In general, the canonical performance of the system in Fig. 5(a) in a quasi-static fading channel is defined as the performance of the reference system in Fig. 5(b) averaged over $\boldsymbol{h}$. It can be computed provided that the performance of the FEC code in AWGN channels is known. It serves as a benchmark for the performance of a full transmit diversity system.

E. Performance of IDM-ST Codes

In the following, we will use simulation results to show that IDM-ST codes can nearly achieve the canonical performance. (We are still undertaking an analytical study.)

Let N_{info}, N, S and F be defined as above. Let R_{FEC} be the rate of the FEC code. We define $R_{\text{system}}=F\times R_{\text{FEC}}/S$ as the overall spectrum efficiency. We always assume complex signaling, one receive antenna, and ideal channel state information at the receiver.

Fig. 6 illustrates the performance of IDM-ST schemes without FEC coding over quasi-static single-path Rayleigh fading channels. The performance curves are quite close to their respective canonical performance. By increasing N from 2 to 16, substantial gain (about 15dB) is achieved (measured at BER=10^{-5}). For N>2, the performance in Fig. 6 is also considerably better than that of existing schemes [4][5].

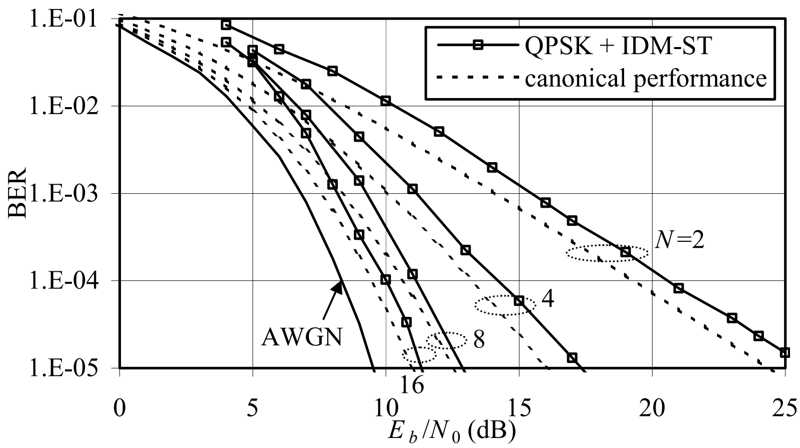

Fig. 6. Performance of uncoded IDM-ST schemes over quasi-static single-path Rayleigh fading channels. S=(8, 4, 2, 1) for N=(2, 4, 8, 16). F=2S. R_{system}=2 bits/symbol. No ISI. N_{info}=512. Iteration number=10.

Fig. 7 illustrates the performance of IDM-ST schemes with rate-½ convolutional coding over quasi-static single-path Rayleigh fading channels. We can see that these schemes can nearly achieve the canonical performance at BER=10^{-5}. It appears that FEC coding can facilitate the iterative process at the receiver as now the APP decoding in DEC can provide more reliable feedback information to the GCD.

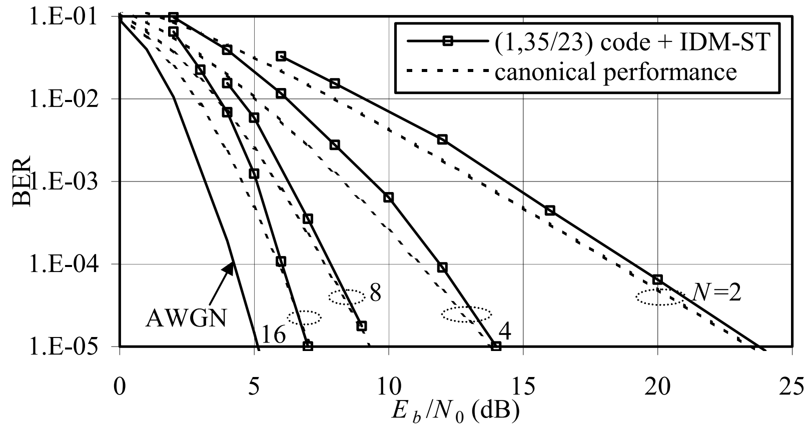

Fig. 7. Performance of convolutionally coded IDM-ST schemes over quasi-static single-path Rayleigh fading channels. Generators = $(1, 35/23)_8$. R_{FEC}=1/2. S=2. F=4. R_{system}=1 bit/symbol. No ISI. N_{info} =1000. Iteration number=5.

Fig. 8 shows the performance of convolutionally coded IDM-ST schemes in a quasi-static multipath Rayleigh fading channel. The canonical performance curves for single-path channels are also included for reference. We can see that the IDM-ST schemes can efficiently exploit multipath diversity, e.g., an N = 2 IDM-ST scheme in a 4-tap multipath channel can achieve nearly the same performance of an N = 8 system in a single-path channel.

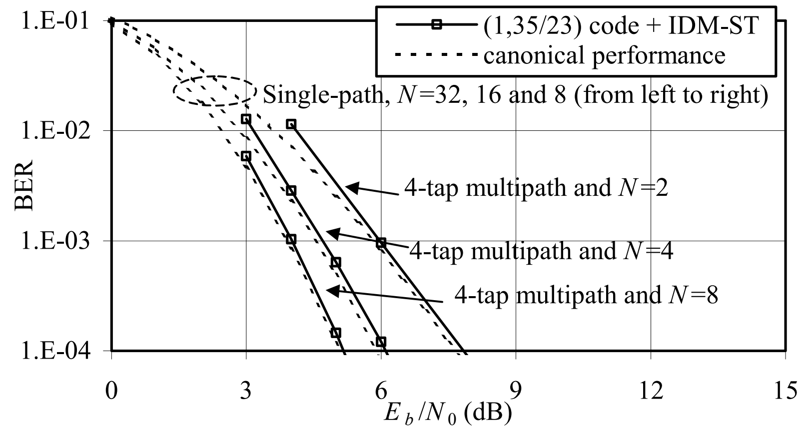

Fig. 8. Performance of convolutionally coded IDM-ST schemes over a 4-tap multipath channel. Generators=$(1, 35/23)_8$. R_{FEC}=1/2. F=S=2. R_{system}=0.5 bits/symbol. Four tap coefficients have the same variance. N_{info}=1000. Iteration number=5.

IV. Conclusions

Interleave-based schemes have been introduced for multiuser detection and space-time coding. Simulation results have been provided to show that such schemes can achieve nearly optimal performance at very low receiver costs in both cases.

Appendix: A Generalized Tanner Graph Approach

In [17], a very inspiring multiuser detection scheme is described using Tanner graphs (TGs). We now show that the principle in [17] can be generalized and applied to both CDMA and IDMA schemes. This helps to gain more insights into their similarities and differences.

A. Generalized Tanner Graphs

The generalized Tanner graphs (GTGs) for CDMA and IDMA systems given in Fig. 9 consist of variable nodes (black nodes) for transmitted chips $\{x_j^{(m)}\}$, observation nodes (dashed ovals) for observations $\{r_j\}$ and constraint nodes (squares) for the relationship that all chips connecting to a common constraint node belong to the same frame of a spreading sequence. For simplicity, some extremely simplified parameters are used here:

- User number $M = 2$ and no ISI (see (1)).
- No FEC code (so each variable node is connected to only one constraint node representing a spreading relationship).

The principle can easily be generalized to systems with more users.

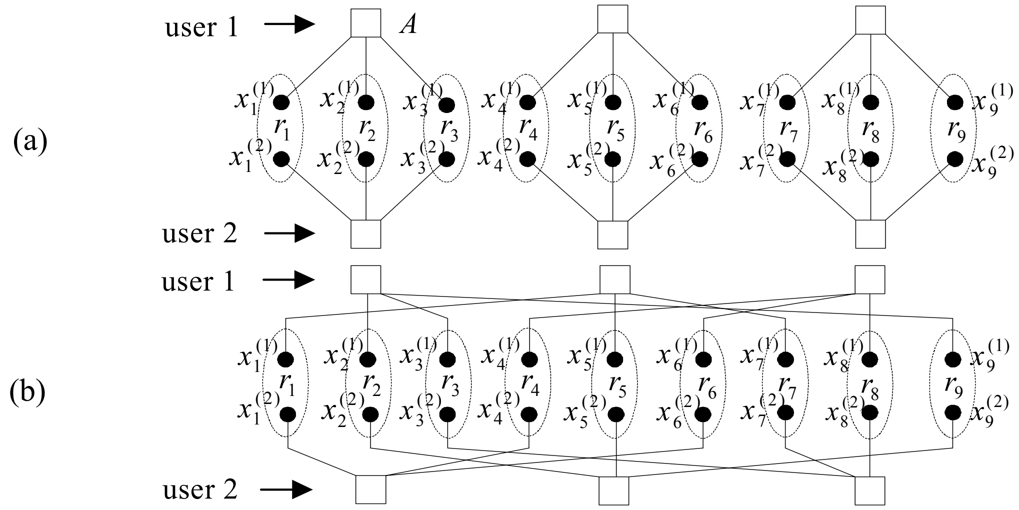

Fig. 9. (a) A GTG for a conventional CDMA scheme and (b) a GTG for an IDMA scheme, where the black nodes inside an oval are related by $r_j = h^{(1)}x_j^{(1)} + h^{(2)}x_j^{(2)} + n_j$, i.e., equation (1) with $M = 2$. Spreading length $S = 3$. Notice that (a) and (b) are different only in the connection of edges.

B. Message Passing Decoding based on GTGs

We can derive a message passing detection algorithm for a GTG similar to that used for a TG [18]. Two types of messages are defined:

- A message from a variable node to a constraint node is defined as $L(x_j^{(m)})$.
- A message from a constraint node to a variable node is defined as $Ext(x_j^{(m)})$.

The operations on variable nodes involve (12)–(14) for generating $\{L(x_j^{(m)})\}$ and those on constraint nodes involve the APP decoding for generating $\{Ext(x_j^{(m)})\}$.

The main difference between the GTG in Fig. 9 and the TG used in [17] is at the constraint nodes. In [17], each constraint node represents a single-parity-check relationship. For the GTG in Fig. 9, each constraint node represents a spreading operation. For example, let $\boldsymbol{s}=[s_1, s_2, s_3]$ be the spreading sequence for user-1 in Fig. 9(a). Let the spreading operation be $c_1 \rightarrow c_1 \cdot \boldsymbol{s}$ where c_1 is the first bit to be spread. The values of the variable nodes connected to constraint node A in Fig. 9(a) are given as: $x_1^{(1)} = c_1 \cdot s_1$, $x_2^{(1)} = c_1 \cdot s_2$ and $x_3^{(1)} = c_1 \cdot s_3$. Therefore the constraint represented by A is

$$x_1^{(1)} / s_1 = x_2^{(1)} / s_2 = x_3^{(1)} / s_3 .$$

This represents a much stronger constraint than the single-parity-check relationship. It makes the systems in Fig. 9 more robust against interference, so that a large number of users can be supported.

C. The Difference between Conventional CDMA and IDMA

The difference between CDMA and IDMA is at edge connections. In a conventional synchronous CDMA, a frame of one user will overlap a frame of another user. This results in short cycles in the GTG (see Fig. 9(a)), which have a detrimental effect in a message passing process [18]. For IDMA, the randomized edge connection greatly reduces the number of short cycles (see Fig. 9(b)). This is essential for the success of a message passing process [19].

Acknowledgement

The authors are deeply indebted to Peter Hoeher for his many insightful suggestions and enlightening discussions.

References

[1] M. Moher, "An iterative multiuser decoder for near-capacity communications," *IEEE Trans. Commun.*, vol. 46, pp. 870–880, July 1998.

[2] M. C. Reed, C. B. Schlegel, P. D. Alexander, and J. A. Asenstorfer, "Iterative multiuser detection for CDMA with FEC: Near-single-user performance," *IEEE Trans. Commun.*, vol. 46, pp. 1693–1699, Dec. 1998.

[3] X. Wang and H. V. Poor, "Iterative (turbo) soft interference cancellation and decoding for coded CDMA," *IEEE Trans. Commun.*, vol. 47, pp. 1046–1061, July 1999.

[4] V. Tarokh, N. Seshadri, and A. R. Calderbank, "Space-time codes for high data rate wireless communication: Performance analysis and code consruction," *IEEE Trans. Inform. Theory*, vol. 44, pp. 744-765, Mar. 1998.

[5] V. Tarokh, H. Jafarkhani, and A. R. Calderbank, "Space-time block codes from orthogonal designs," *IEEE Trans. Inform. Theory*, vol. 45, pp. 1456-1467, July 1999.

[6] S. Brück, U. Sorger, S. Gligorevic, and N. Stolte, "Interleaving for outer convolutional codes in DS-CDMA Systems," *IEEE Trans. Commun.*, vol. 48, pp. 1100–1107, July 2000.

[7] A. Tarable, G. Montorsi, and S. Benedetto, "Analysis and design of interleavers for CDMA systems," *IEEE Commun. Lett.*, vol. 5, pp. 420–422, Oct. 2001.

[8] F. N. Brannstrom, T. M. Aulin, and L. K. Rasmussen, "Iterative multi-user detection of trellis code multiple access using a posteriori probabilities," in *Proc. ICC 2001*, Finland, June 2001, pp. 11–15.

[9] P. Frenger, P. Orten, and T. Ottosson, "Code-spread CDMA using maximum free distance low-rate convolutional codes," *IEEE Trans. Commun.*, vol. 48, pp. 135–144, Jan. 2000.

[10] Li Ping, W. K. Leung, and K. Y. Wu, "Low-rate turbo-Hadamard codes," submitted for publication (www.ee.cityu.edu.hk/~liping).

[11] C. Berrou and A. Glavieux, "Near Shannon limit error correcting coding and decoding: Turbo-codes," *IEEE Trans. Commun.*, vol. 44, pp. 1261–1271, Oct. 1996.

[12] Z. Shi and C. Schlegel, "Joint iterative decoding of serially concatenated error control coded CDMA," *IEEE J. Select. Areas Commun.* vol. 19, pp. 1646–1653, Aug. 2001.

[13] S. Verdú, "The capacity region of the symbol-asynchronous Gaussian multiple-access channel," *IEEE Trans. Inform. Theory*, vol. 35, pp. 733-751, July 1989.

[14] A. Narula, M. D. Trott, and G.W. Wornell, "Performance limits of coded diversity methods for transmitter antenna arrays," *IEEE Trans. Inform. Theory*, vol. 45, pp. 2418-2433, Nov. 1999.

[15] G. J. Foschini and M. Gans, "On the limits of wireless communication in a fading environment when using multiple antennas," *Wireless Personal Commun*., vol. 6, pp. 311-335, Mar. 1998.

[16] J. G. Proakis, *Digital Communications*. McGraw-Hill, 1995.

[17] R. McEliece, "Are turbo-like codes effective on nonstandard channels?" *IEEE Inform. Theory Society Newsletter*, vol. 51, pp. 1-8, Dec. 2001.

[18] F. E. Kschischang, B. J. Frey, and H.-A. Loeliger, "Factor graphs and the sum-product algorithm," *IEEE Trans. Inform. Theory*, vol. 47, pp. 498–519, Feb. 2001.

[19] Y. Mao and A. H. Banihashemi, "A heuristic search for good low-density parity-check codes at short block lengths," in *Proc. ICC 2001*, Finland, June 2001, pp. 41–44.